Ultra Scientist Vol. 25(1)B, 17-34 (2013).

Effects of slip and heat transfer on the peristaltic flow of MHD Carreau fluid

*Y. RAJESH YADAV and **V. VASU

(Acceptance Date 24th January, 2013)

Abstract

Effects of slip and heat transfer on the peristaltic flow of MHD Carreau fluid is studied under long wave length and low Reynolds number assumptions. The channel asymmetry produced by choosing the different peristaltic wave train likely sinusoidal, triangle, square, trapezoidal and sawtooth. The nonlinear governing equations are solved using a perturbation technique based on small Weissenberg number. Expressions for the stream function, pressure gradient, temperature distribution, axial induced magnetic force function and shear stress on the wall are obtained. The effects of different parameters entering into problem are discussed numerically and explained graphically. We concluded that size of the bolus decreases with increasing Hartmann number M and partial slip β .

1. Introduction

There has been a recent interest in peristaltic pumping which can produce a flow in a duct completely isolated from the pump of mechanism. Roller pumps, used to pump blood, food or corrosive liquids operate under the principle. Considerable analysis of this mechanism has been carried out, primarily for a Newtonian fluid with a periodic train of sinusoidal peristaltic waves. The inertia free peristaltic flow with a long wavelength at low Reynolds number analysis was given by Shapiro *et al.*[1]. Peristaltic transport of blood in small vessels was investigated using the viscoelastic, power-law, micropolar, Casson fluid etc, models by [2-10]. However in Refs.[11–14], the authors have analyzed the interaction of slip and the heat transfer on the peristalsis.

Very recently, the combined effects of heat transfer and magnetic field on the peristaltic transport of a Carreau fluid have been discussed in Ref.[25]. The existing literature indicates that the heat transfer and magnetic field characteristics on the peristalsis have not

been discussed so far when no-slip condition is no longer valid. In all these previous investigations authors have discussed the velocity field, pressure gradient, pressure rise and heat transfer distribution but they did not study the different wave forms and shear stress on the peristaltic flow of a Carreau fluid.

In this paper, we study the steady incompressible MHD Carreau fluid flow in an asymmetric channel under the effects of slip and heat transfer with long wavelength and low Reynolds number assumptions. The problem examined numerically using perturbation technique by small Weissenberg number, which provides an effective computation tool for the solution of nonlinear equations. The influence of different parameters on axial velocity, pressure gradient, pressure rise, shear stress, axial induced magnetic field, temperature distribution, trapping and different wave forms phenomena are studied and discussed graphically[15-20].

2. Mathematical formulation :

Let us consider the peristaltic transport of an incompressible Carreau fluid under the effect of magnetic field in a two–dimensional channel of width $d_1 + d_2$ .The flow is generated by sinusoidal wave trains propagating with constant speed c along the asymmetric channel. The geometry of the wall surfaces is defined as

$$h_1\left(\bar{X},\bar{t}\right)=\bar{d}_1+\bar{a}_1\cos\left[\frac{2\pi}{\lambda}\left(\bar{X}-c\bar{t}\right)\right] \quad \text{.....}$$

upper wall (1)

$$h_2\left(\bar{X},\bar{t}\right)=-\bar{d}_2-\bar{a}_2\cos\left[\frac{2\pi}{\lambda}\left(\bar{X}-c\bar{t}\right)+\phi\right] \quad \text{.....}$$

lower wall (2)

in which $\bar{a}_1$ and $\bar{a}_2$ are the amplitudes of the waves, λ is the wave length, *c* is the wave speed, ϕ $(0 \le \phi \le \pi)$ is the phase difference, $\bar{X}$ and $\bar{Y}$ are the rectangular coordinates with $\bar{X}$ measured along the axis of the channel and $\bar{Y}$ **is** perpendicular to $\bar{X}$. Let $(\bar{U},\bar{V})$ be the velocity components in fixed frame of reference $(\bar{X},\bar{Y})$. It should be noted that $\phi = 0$ it corresponds to symmetric channel with waves out of phase and for $\phi = \pi$ the waves are in phase. Furthermore, $\bar{a}_1$, $\bar{a}_2$, $\bar{d}_1$, $\bar{d}_2$ and ϕ satisfy the condition

$$\bar{a}_1^{\,2}+\bar{a}_2^{\,2}+2\bar{a}_1\bar{a}_2\cos\phi\le\left(\bar{d}_1+\bar{d}_2\right)^2. \qquad (3)$$

Introducing a wave frame $(\bar{x},\bar{y})$ moving with velocity *c* away from the fixed frame $(\bar{X},\bar{Y})$ by the transformation

$$\bar{x}=\bar{X}-c\bar{t},\ \ \bar{y}=\bar{Y},\ \bar{u}\left(\bar{x},\bar{y}\right)=\bar{U}-c,\ \bar{v}\left(\bar{x},\bar{y}\right)=\bar{V}. \qquad (4)$$

3. Equations of motion :

The governing equations governing the flow in the present problem are[25]

A constant magnetic field of the strength $\bar{H}_0$ is applied in the transverse direction. This gives rise to an induced magnetic field $\bar{H}^+\left(\bar{h}_{\bar{x}}\left(\bar{X},\bar{Y},\bar{t}\right),\ \bar{h}_{\bar{y}}\left(\bar{X},\bar{Y},\bar{t}\right),\ 0\right)$ and hence the total magnetic field become $\bar{H}^+\left(\bar{h}_{\bar{x}}\left(\bar{X},\bar{Y},\bar{t}\right).\bar{H}_0+\bar{h}_{\bar{y}}\left(\bar{X},\bar{Y},\bar{t}\right),\ 0\right)$.

$$\nabla.\,\bar{\mathbf{H}}=0,\ \ \nabla.\,\bar{\varepsilon}=0, \qquad (5)$$

$$\nabla\times\bar{\mathbf{H}}=\bar{\mathbf{J}},\ \ \bar{\mathbf{J}}=\sigma\left\{\bar{\varepsilon}+\mu_e\left(\bar{\mathbf{V}}'\ \bar{\mathbf{H}}\right)\right\}, \qquad (6)$$

$$\nabla\times\bar{\varepsilon}=-\mu_e\frac{\partial\bar{\mathrm{H}}}{\partial\bar{\mathrm{t}}}, \qquad (7)$$

$$\nabla \cdot \bar{\mathbf{V}}' = 0, \tag{8}$$

$$\rho\left(\frac{\partial}{\partial \bar{t}} + (\bar{\mathbf{V}} \cdot \nabla)\right)\bar{\mathbf{V}}' = -\nabla \bar{p} + \operatorname{div} \bar{t}' - \mu_e \bar{\mathbf{H}}^{+} \cdot \nabla \bar{\mathbf{H}}^{+} - \frac{1}{2}\left|\bar{\mathbf{H}}^{+}\right|^2 \nabla, \tag{9}$$

$$\rho C_p \frac{dT}{dt} = \kappa \nabla^2 T + \tau_1 \cdot \mathbf{L}. \tag{10}$$

In the above expresses ions τ_1 is the Cauchy stress tensor. $\mathbf{L}$ = grad$\mathbf{V}$, $\bar{p}$ is the pressure, $\bar{\mathbf{H}}$ is the induced magnetic field, $\bar{\mathbf{J}}$ the current density, μ_e magnetic permeability, σ the electrical conductivity, $\bar{\varepsilon}$ electrical field, C_p the specific heat at a constant volume, κ the thermal conductivity and temperature. The velocity $\bar{\mathbf{V}}$ is defined by

$$\bar{V} = (\bar{u}, \bar{v}, 0). \tag{11}$$

The constitutive equation for a Carreau fluid is

$$\bar{\tau} = -\left[\eta_\infty + (\eta_0 - \eta_\infty)\left(1 + (\Gamma \bar{\dot{\gamma}})^2\right)^{\frac{n-1}{2}}\right]\bar{\dot{\gamma}}, \tag{12}$$

where τ is the extra stress tensor, η_∞ is the infinite shear rate viscosity, η_0 is the zero shear-rate viscosity, Γ is the time constant, n is the dimensionless power law index. The above model reduces to Newtonian Model for n=1 or Γ=0 and $\dot{\gamma}$ is defined as

$$\bar{\dot{\gamma}} = \sqrt{\frac{1}{2}\sum_i \sum_j \bar{\dot{\gamma}}_{ij} \bar{\dot{\gamma}}_{ji}} = \sqrt{\frac{1}{2}\Pi} \tag{13}$$

Induction equation after using Eqs. (5)-(8) take the form

$$\frac{\partial \bar{\mathbf{H}}}{\partial \bar{t}} = \nabla \times \left\{\bar{\mathbf{V}} \times \bar{\mathbf{H}}^{+}\right\} + \frac{1}{\zeta}\nabla^2 \bar{\mathbf{H}}^{+}. \tag{14}$$

in which $\zeta = \dfrac{1}{\sigma \mu_e}$ is magnetic diffusity.

The following non-dimension quantities are also defined

$$x = \frac{\bar{x}}{\lambda},\ y = \frac{\bar{y}}{\bar{d}_1},\ u = \frac{\bar{u}}{c},\ v = \frac{\bar{v}}{c},\ t = \frac{c}{\lambda}\bar{t},\ h_1 = \frac{\bar{h}_1}{\bar{d}_1},$$

$$h_2 = \frac{\bar{h}_2}{\bar{d}_1},\ \tau = \frac{\bar{d}_1}{\mu c}\bar{\tau},\ \Phi = \frac{\bar{\Phi}}{H_0 \bar{d}_1},\ S_t = \frac{H_0}{C}\sqrt{\frac{\mu_e}{\rho}},$$

$$\dot{\gamma} = \frac{\bar{\dot{\gamma}}\bar{d}_1}{c},\ \delta = \frac{\bar{d}_1}{\lambda},\ We = \frac{\Gamma c}{d_1},\ p = \frac{\bar{d}_1^{\,2}}{c\lambda\mu}\bar{p},\ \mathrm{Re} = \frac{\rho c \bar{d}_1}{\mu},$$

$$M = \sqrt{\frac{\sigma}{\mu}} B_0 d_1,\ R_m = \sigma \mu_e a c,\ P_r = \frac{\rho \nu C_p}{\kappa},$$

$$\theta = \frac{T - T_0}{T_1 - T_0},\ E = \frac{c^2}{C_p (T_1 - T_0)},\ \psi = \frac{\bar{\psi}}{c\bar{d}_1},\ a = \frac{\bar{a}_1}{\bar{d}_1},$$

$$b = \frac{\bar{a}_2}{\bar{d}_1},\ d = \frac{\bar{d}_2}{\bar{d}_1}. \tag{15}$$

Using the above non-dimensional quantities have given in the Eqs. (9) and (14), the resulting equations in terms of stream function can be written as

$$\mathrm{Re}\,\delta\left\{\left(\frac{\partial \psi}{\partial y}\frac{\partial}{\partial x} - \frac{\partial \psi}{\partial x}\frac{\partial}{\partial y}\right)\frac{\partial \psi}{\partial y}\right\} = -\frac{\partial p_m}{\partial x} + \delta\frac{\partial \tau_{xx}}{\partial x} + \frac{\partial \tau_{xy}}{\partial y}$$

$$+ \mathrm{Re}\,\delta S_t^2\left(\frac{\partial \phi}{\partial y}\frac{\partial}{\partial x} - \frac{\partial \phi}{\partial x}\frac{\partial}{\partial y}\right)\frac{\partial \phi}{\partial y} + \mathrm{Re}\,S_t^2\frac{\partial^2 \phi}{\partial y^2}, \tag{16}$$

$$-\mathrm{Re}\,\delta^3\left\{\left(\frac{\partial \psi}{\partial y}\frac{\partial}{\partial x} - \frac{\partial \psi}{\partial x}\frac{\partial}{\partial y}\right)\frac{\partial \psi}{\partial x}\right\} = -\frac{\partial p_m}{\partial y} + \delta^2\frac{\partial \tau_{xy}}{\partial x}$$

$$+ \delta\frac{\partial \tau_{yy}}{\partial x} - \mathrm{Re}\,\delta^3 S_t^2\left(\frac{\partial \phi}{\partial y}\frac{\partial}{\partial x} - \frac{\partial \phi}{\partial x}\frac{\partial}{\partial y}\right)\frac{\partial \phi}{\partial x} - \mathrm{Re}\,\delta^2 S_t^2\frac{\partial^2 \phi}{\partial x \partial y}, \tag{17}$$

$$\frac{\partial \psi}{\partial y} - \delta\left(\frac{\partial \psi}{\partial y}\frac{\partial \phi}{\partial x} - \frac{\partial \psi}{\partial x}\frac{\partial \phi}{\partial y}\right) + \frac{1}{R_m}\nabla^2 \Phi = E, \tag{18}$$

$$\frac{\partial^2 \theta}{\partial y^2} + Br\left\{1 + \frac{(n-1)}{2}We^2\dot{\gamma}^2\right\}\left(\frac{\partial^2 \psi}{\partial y^2} - \delta^2\frac{\partial^2 \psi}{\partial x^2}\right)\frac{\partial^2 \psi}{\partial y^2} = 0, \tag{19}$$

where

$$u=\frac{\partial\psi}{\partial y},\quad \upsilon=-\delta\frac{\partial\psi}{\partial x},\quad \mathrm{h}_x=\frac{\partial\phi}{\partial y},\quad \mathrm{h}_y$$

$$=-\delta\frac{\partial\phi}{\partial x},\quad \mathrm{Br=EPr}, \tag{20}$$

$$p_m=p+\frac{1}{2}\mathrm{Re}\,\delta\frac{\mu_e\left(H^{'-}\right)^2}{\rho c^2}, \tag{21}$$

$$\nabla^2=\delta^2\frac{\partial^2}{\partial^2 x}+\frac{\partial^2}{\partial y^2}, \tag{22}$$

$$\tau_{xx}=-2\left[1+\frac{(n-1)}{2}We^2\dot{\gamma}^2\right]\frac{\partial^2\psi}{\partial x\partial y}, \tag{23}$$

$$\tau_{xy}=-\left[1+\frac{(n-1)}{2}We^2\dot{\gamma}^2\right]\left(\frac{\partial^2\psi}{\partial y^2}-\delta^2\frac{\partial^2\psi}{\partial x^2}\right), \tag{24}$$

$$\tau_{yy}=2\delta\left[1+\frac{(n-1)}{2}We^2\dot{\gamma}^2\right]\frac{\partial^2\psi}{\partial x\partial y}, \tag{25}$$

$$\dot{\gamma}=\left[2\delta^2\left(\frac{\partial^2\psi}{\partial x\partial y}\right)^2+\left(\frac{\partial^2\psi}{\partial y^2}-\delta^2\frac{\partial^2\psi}{\partial x^2}\right)+2\delta^2\left(\frac{\partial^2\psi}{\partial x\partial y}\right)^2\right]^{\frac{1}{2}}. \tag{26}$$

Here δ is a wave number, Re the Reynolds number, R_m the magnetic Reynolds number, S_t the Strommer's number, p_m the magnetic pressure, *We* the Weissenberg number, *M* the Hartman number, Pr the Prandtl number, *E* the Eckert number and *Br* the Brickman number[21-24].

Eqs. (16) - (19) after invoking long wave length and low Reynolds number assumptions reduce to

$$\frac{\partial p}{\partial x}=\frac{\partial}{\partial y}\left[\left\{1+\frac{(n-1)}{2}We^2\left(\frac{\partial^2\psi}{\partial y^2}\right)^2\right\}\frac{\partial^2\psi}{\partial y^2}\right]+M^2\left(\varepsilon-\frac{\partial\psi}{\partial y}\right), \tag{27}$$

$$\frac{\partial p}{\partial y}=0, \tag{28}$$

$$\frac{\partial\psi}{\partial y}+\frac{1}{R_m}\frac{\partial^2\Phi}{\partial y^2}=E,\ \frac{\partial^2\theta}{\partial y^2}+Br\left[\left\{1+\frac{(n-1)}{2}We^2\left(\frac{\partial^2\psi}{\partial y^2}\right)^2\right\}\left(\frac{\partial^2\psi}{\partial y^2}\right)^2\right]=0. \tag{29}$$

$$\frac{\partial^2}{\partial y^2}\left[\left\{1+\frac{(n-1)}{2}We^2\left(\frac{\partial^2\psi}{\partial y^2}\right)^2\right\}\frac{\partial^2\psi}{\partial y^2}\right]-M^2\frac{\partial^2\psi}{\partial y^2}=0. \tag{30}$$

4. Boundary conditions :

In the wave frame, the boundary conditions are

$$\psi=\frac{q}{2},\ \frac{\partial\psi}{\partial y}+\beta\frac{\partial^2\psi}{\partial y^2}=-1,\ \theta=0,\ \Phi=0\ at$$

$$y=h_1=1+a\cos 2\pi x, \tag{31}$$

$$\psi=-\frac{q}{2},\ \frac{\partial\psi}{\partial y}-\beta\frac{\partial^2\psi}{\partial y^2}=-1,\ \theta=1,\ \Phi=0\ at$$

$$y=h_2=-d-b\cos\left(2\pi x+\phi\right). \tag{32}$$

The dimensionless mean flow rate in laboratory $\bar{Q}$ and wave frame *F* are related by the following expression

$$\bar{Q}=F+d+1. \tag{33}$$

in which

$$F=\int_{h_2(x)}^{h1(x)}\frac{\partial\psi}{\partial y}dy=\psi\left(h_1(x)\right)-\psi\left(h_2(x)\right).$$

5. Perturbation solution :

For perturbation solution, we expand, ψ, q, p and Φ as

$$\psi=\psi_0+We^2\psi_1+O\left(We^4\right), \tag{34}$$

$$q=q_0+We^2q_1+O\left(We^4\right), \tag{35}$$

$$p=p_0+We^2p_1+O\left(We^4\right). \tag{36}$$

$$\Phi=\Phi_0+We^2\Phi_1+O\left(We^4\right). \tag{37}$$

The perturbation series solution up to second order for stream function ψ, pressure gradient $\frac{dp}{dx}$, pressure rise ΔP_λ, magnetic force function Φ and shear stress τ_{xy} can be summarized as

$$\begin{aligned}\psi &= C_1 + C_2 y + C_3 \cosh My + C_4 \sinh My \\ &\quad + We^2\Big[C_5 + C_6 y + C_7 \cosh My + C_8 \sinh My \\ &\qquad - \frac{M^4}{64}(n-1)\Big(C_3\left(C_3^2+3C_4^2\right)\cosh 3My + C_4\left(C_4^2+3C_3^2\right)\sinh 3My\Big) \\ &\qquad - \frac{3}{16}M^5(n-1)\left(C_3^2-C_4^3\right)\Big(\left(2C_3+MC_4y\right)\cosh My + \left(MC_3y+2C_4\right)\sinh My\Big)\Big],\end{aligned} \tag{38}$$

$$\begin{aligned}\frac{dp}{dx} &= M^2\varepsilon + \frac{M^2\left[\left(2+M^2q\beta\right)\sinh M\left(\frac{h_1-h_2}{2}\right)+Mq\cosh M\left(\frac{h_1-h_2}{2}\right)\right]}{\left[\left(2-M^2\beta\left(h_1-h_2\right)\right)\sinh M\left(\frac{h_1-h_2}{2}\right)\right]-M(h_1-h_2)\cosh M\left(\frac{h_1-h_2}{2}\right)} \\ &\quad - We^2\left[\frac{M^2}{(h_1-h_2)}\left(q-\frac{qL_5}{(h_1-h_2)L_7}-\frac{L_8L_5}{L_7}-L_6\right)\right],\end{aligned} \tag{39}$$

$$\Delta P_\lambda = \int_0^{2\pi}\frac{dp}{dx}dx, \tag{40}$$

$$\begin{aligned}\theta &= -\frac{M^2Br}{8}\left(C_3^2+C_4^2\right)\cosh 2My - \frac{M^2Br}{4}C_3C_4\sinh 2My - \frac{M^4Br}{4}\left(C_4^2-C_3^2\right)y^2 + C_9y + C_{10} \\ &\quad - We^2\Bigg[Br\Bigg(\left(2\left(L_9+L_{10}y-\frac{L_{12}}{M}\right)+\frac{(n-1)}{4}\left(C_3^4-C_4^4\right)\right)\frac{\cosh 2My}{4M^2} \\ &\qquad + \left(2\left(L_{11}+L_{12}y-\frac{L_{10}}{M}\right)+\frac{(n-1)}{2}C_3C_4\left(C_3^2-C_4^2\right)\right)\frac{\sinh 2My}{4M^2} \\ &\qquad + \left(2L_{13}+\frac{(n-1)}{16}\left(C_3^4+C_4^4+6C_3^2C_4^2\right)\right)\frac{\cosh 4My}{16M^2} + \left(2L_{14}+\frac{(n-1)}{4}C_3C_4\left(C_3^2+C_4^2\right)\right)\frac{\sinh 4My}{16M^2} \\ &\qquad + \left(2L_{15}+\frac{3}{8}\left(C_3^2-C_4^2\right)^2\right)\frac{y^2}{2}\Bigg) - C_{11}y - C_{12}\Bigg],\end{aligned} \tag{41}$$

$$\begin{aligned}\Phi &= R_m\left(\left(E-C_2\right)\frac{y^2}{2} - \frac{C_3}{M}\sinh My - \frac{C_4}{M}\cosh My\right) + C_{13}y + C_{14} \\ &\quad - We^2\Bigg[R_m\Bigg(C_6\frac{y^2}{2} + \frac{C_7}{M}\sinh My + \frac{C_8}{M}\cosh My \\ &\qquad - \frac{(n-1)}{192}M^3\left(C_3\left(C_3^2+3C_4^2\right)\sinh 3My + C_4\left(C_4^2+3C_3^2\right)\cosh 3My\right) \\ &\qquad - \frac{3(n-1)}{16}M^3\left(C_3^2-C_4^2\right)\begin{pmatrix}M\left(C_3y\cosh My + C_4y\sinh My\right)\\ -\left(C_3\sinh My + C_4\cosh My\right)\end{pmatrix} - C_{15}y - C_{16}\Bigg],\end{aligned} \tag{42}$$

$$\tau_{xy} = -M^2 C_3 \cosh My - M^2 C_4 \sinh My - We^2 \left[\frac{(n-1)}{2} \left(M^2 C_3 \cosh My + M^2 C_4 \sinh My \right)^3 \right.$$
$$- \frac{9}{64} M^6 (n-1) \left(C_3 \left(C_3^2 + 3C_4^2 \right) \cosh 3My + C_4 \left(C_4^2 + 3C_3^2 \right) \sinh 3My \right)$$
$$+ M^2 C_7 \cosh My + M^2 C_8 \sinh My \qquad (43)$$
$$\left. - \frac{3}{16} M^6 (n-1) \left(C_3^2 - C_4^2 \right) \left((2C_3 + MC_4 y) \cosh My + (MC_3 y + 2C_4) \sinh My \right) \right]$$

were

$$C_1 = \frac{q}{2} + \frac{Mqh_1 \cosh M\left(\frac{h_1 - h_2}{2}\right) + \left[\left(2 + M^2 q\beta\right) h_1 - \left(q + h_1 - h_2\right) \right] \sinh M\left(\frac{h_1 - h_2}{2}\right)}{\left[2 - M^2 \beta \left(h_1 - h_2\right)\right] \sinh M\left(\frac{h_1 - h_2}{2}\right) - M\left(h_1 - h_2\right) \cosh M\left(\frac{h_1 - h_2}{2}\right)},$$

$$C_2 = -\frac{\left[\left(2 + M^2 q\beta\right) \sinh M\left(\frac{h_1 - h_2}{2}\right) + Mq \cosh M\left(\frac{h_1 - h_2}{2}\right) \right]}{\left[\left(2 - M^2 \beta \left(h_1 - h_2\right)\right) \sinh M\left(\frac{h_1 - h_2}{2}\right) \right] - M\left(h_1 - h_2\right) \cosh M\left(\frac{h_1 - h_2}{2}\right)},$$

$$C_3 = -\frac{\left[\left(q + h_1 - h_2\right) \sinh M\left(\frac{h_1 + h_2}{2}\right) \right]}{\left[2 - M^2 \beta \left(h_1 - h_2\right)\right] \sinh M\left(\frac{h_1 - h_2}{2}\right) - M\left(h_1 - h_2\right) \cosh M\left(\frac{h_1 - h_2}{2}\right)},$$

$$C_4 = \frac{\left(q + h_1 - h_2\right) \cosh M\left(\frac{h_1 + h_2}{2}\right)}{\left[2 - M^2 \beta \left(h_1 - h_2\right)\right] \sinh M\left(\frac{h_1 - h_2}{2}\right) - M\left(h_1 - h_2\right) \cosh M\left(\frac{h_1 - h_2}{2}\right)},$$

$$C_5 = \frac{q}{2} + \frac{h_1}{\left(h_1 - h_2\right)} \left(\frac{qL_5}{L_7} + \frac{L_8 L_5}{\left(h_1 - h_2\right) L_7} + L_6 - q \right) - \frac{\sinh Mh_1}{L_7} \left(\frac{q}{h_1 - h_2} + L_8 \right)$$
$$+ \frac{\cosh Mh_1}{M\left(\sinh Mh_1 - \sinh Mh_2\right)} \left(\frac{M}{L_7} \left(\cosh Mh_1 - \cosh Mh_2 \right) \left(\frac{q}{h_1 - h_2} + L_8 \right) + L_3 - L_4 \right) - L_1,$$

$$C_6 = \frac{1}{(h_1 - h_2)}\left(q - \frac{qL_5}{(h_1 - h_2)L_7} - \frac{L_8 L_5}{L_7} - L_6 \right),$$

$$C_7 = \frac{-1}{(\sinh Mh_1 - \sin M\, \mathrm{h}_2)}\left(\frac{(\cosh Mh_1 - \cosh Mh_2)}{L_7}\left(\frac{q}{(h_1 - h_2)} + L_8 \right) + \frac{(L_3 - L_4)}{M} \right),$$

$$C_8 = \frac{1}{L_7}\left(\frac{q}{(h_1 - h_2)} + L_8 \right),$$

$$C_9 = \frac{1}{(h_2 - h_1)}\left(1 - \frac{BrM^2}{8}\begin{pmatrix} (C_3^2 + C_4^2)(Cosh2Mh_1 - \cosh 2Mh_2) + 2(C_4^2 - C_3^2)(h_1^2 - h_2^2) \\ +2C_3C_4(\sinh 2Mh_1 - \sinh 2Mh_2) \end{pmatrix} \right),$$

$$C_{10} = \frac{1}{(h_1 - h_2)}\left(h_1 - \frac{BrM^2}{8}\begin{pmatrix} (C_3^2 + C_4^2)(h_2 Cosh2Mh_1 - h_1 \cosh 2Mh_2) + 2(C_4^2 - C_3^2)h_1h_2(h_1^2 - h_2^2) \\ +2C_3C_4(h_2 \sinh 2Mh_1 - h_1 \sinh 2Mh_2) \end{pmatrix} \right),$$

$$\begin{aligned} C_{11} = -Br\Bigg[& \left(2\left(L_9 - \frac{L_{12}}{M} \right) + \frac{(n-1)}{2}L_{16} \right)\frac{1}{4M^2}(\cosh 2Mh_2 - \cosh 2Mh_1) + \frac{L_{10}}{2M^2}(h_2 \cosh 2Mh_2 - h_1 \cos 2Mh_1) \\ & + \left(2\left(L_{11} - \frac{L_{10}}{M} \right) + \frac{(n-1)}{2}L_{17} \right)\frac{1}{4M^2}(\sinh 2Mh_2 - \sinh 2Mh_1) \\ & + \left(2L_{13} + \frac{(n-1)}{2}L_{18} \right)\frac{1}{16M^2}(\cosh 4Mh_2 - \cosh 4Mh_1) \\ & + \left(2L_{14} + \frac{(n-1)}{2}L_{19} \right)\frac{1}{16M^2}(\sinh 4Mh_2 - \sinh 4Mh_1) + \frac{L_{15}}{3}(h_2^3 - h_1^3) + (2L_{15} + L_{20})\frac{(h_2^2 - h_1^2)}{2} \Bigg], \end{aligned}$$

$$\begin{aligned} C_{12} = -Br\Bigg[& \left(2\left(L_9 - \frac{L_{12}}{M} \right) + \frac{(n-1)}{2}L_{16} \right)\frac{1}{4M^2}(h_2 \cosh 2Mh_1 - h_1 \cosh 2Mh_2) + \frac{L_{10}}{2M^2}h_1h_2(\cosh 2Mh_1 - \cos 2Mh_2) \\ & + \left(2\left(L_{11} - \frac{L_{10}}{M} \right) + \frac{(n-1)}{2}L_{17} \right)\frac{1}{4M^2}(h_2 \sinh 2Mh_1 - h_1 \sinh 2Mh_2) \\ & + \left(2L_{13} + \frac{(n-1)}{2}L_{18} \right)\frac{1}{16M^2}(h_2 \cosh 4Mh_1 - h_1 \cosh 4Mh_2) \\ & + \left(2L_{14} + \frac{(n-1)}{2}L_{19} \right)\frac{1}{16M^2}(h_2 \sinh 4Mh_1 - h_1 \sinh 4Mh_2) + \frac{L_{15}}{3}h_1h_2(h_1^2 - h_2^2) + (2L_{15} + L_{20})\frac{h_1h_2(h_1 - h_2)}{2} \Bigg], \end{aligned}$$

$$C_{13}=\frac{R_m}{(h_2-h_1)}\left((E-C_2)\frac{(h_1^2-h_2^2)}{2}-\frac{C_3}{M}(\sinh Mh_1-\sinh Mh_2)-\frac{C_4}{M}(\cosh Mh_1-\cosh Mh_2)\right),$$

$$C_{14}=\frac{R_m}{(h_1-h_2)}\left((E-C_2)\frac{h_1h_2(h_1-h_2)}{2}-\frac{C_3}{M}(h_2\sinh Mh_1-h_1\sinh Mh_2)-\frac{C_4}{M}(h_2\cosh Mh_1-h_1\cosh Mh_2)\right),$$

$$\begin{aligned}C_{15}=\frac{R_m}{(h_2-h_1)}\Bigg[&C_6\frac{(h_2^2-h_1^2)}{2}+\frac{C_7}{M}(\sinh Mh_2-\sinh Mh_1)+\frac{C_8}{M}(\cosh hMh_2-\cosh Mh_2)\\&-\frac{(n-1)}{192}M^3\left(C_3(C_3^2+3C_4^2)(\sinh 3Mh_2-\sinh 3Mh_1)+C_4(C_4^2+3C_3^2)(\cosh 3Mh_2-\cosh 3Mh_1)\right)\\&-\frac{3(n-1)}{16}M^3(C_3^2-C_4^2)C_3(M(h_2\cosh Mh_2-h_1\cosh Mh_1)-(\sinh Mh_2-\sinh Mh_1))\\&-\frac{3(n-1)}{16}M^3C_4(C_3^2-C_4^2)(M(h_2\sinh Mh_2-h_1\sinh Mh_1)-(\cosh Mh_2-\cosh Mh_1))\Bigg],\end{aligned}$$

$$\begin{aligned}C_{16}=\frac{R_m}{(h_1-h_2)}\Bigg[&C_6\frac{h_1h_2(h_2-h_1)}{2}+\frac{C_7}{M}(h_1\sinh Mh_2-h_2\sinh Mh_1)+\frac{C_8}{M}(h_1\cosh hMh_2-h_1\cosh Mh_2)\\&-\frac{(n-1)}{192}M^3\left(C_3(C_3^2+3C_4^2)(h_1\sinh 3Mh_2-h_2\sinh 3Mh_1)+C_4(C_4^2+3C_3^2)(h_1\cosh Mh_2-h_2\cosh Mh_1)\right)\\&-\frac{3(n-1)}{16}M^4C_3(C_3^2-C_4^2)(Mh_1h_2(\cosh Mh_2-\cosh Mh_1)-(h_1\sinh Mh_2-h_2\sinh Mh_1))\\&-\frac{3(n-1)}{16}M^3C_4(C_3^2-C_4^2)(Mh_1h_2(\sinh Mh_2-\sinh Mh_1)-(h_1\cosh Mh_2-h_2\cosh Mh_1)),\end{aligned}$$

$$\begin{aligned}L_1=&-\frac{M^4}{64}(n-1)\left(C_3(C_3^2+3C_4^2)\cosh 3\mathrm{Mh}_1+C_4(C_4^2+3C_3^2)\sinh 3\mathrm{Mh}_1\right)\\&-\frac{3}{16}M^5(n-1)h_1(C_3^2-C_4^2)(C_3\sinh Mh_1+C_4\cosh Mh_1),\end{aligned}$$

$$\begin{aligned}L_2=&-\frac{M^4}{64}(n-1)\left(C_3(C_3^2+3C_4^2)\cosh 3\mathrm{Mh}_2+C_4(C_4^2+3C_3^2)\sinh 3\mathrm{Mh}_2\right)\\&-\frac{3}{16}M^5(n-1)h_2(C_3^2-C_4^2)(C_3\sinh Mh_2+C_4\cosh Mh_2),\end{aligned}$$

$$L_3=-\frac{3M^5(n-1)}{64}\left(\left(C_3\left(C_3^2+3C_4^2\right)+3\beta MC_4\left(C_4^2+3C_3^2\right)\right)\sinh 3Mh_1+\left(C_4\left(C_4^2+3C_3^2\right)+3\beta MC_3\left(C_3^2+3C_4^2\right)\right)\cosh 3Mh_1\right.$$
$$\left.-\frac{3M^5(n-1)}{16}\left(C_3^2-C_4^2\right)\left(\left((C_3+Mh_1C_4\right)+3\beta M\left(Mh_1C_3+2C_4\right)\right)\sinh Mh_1+\left(\left(Mh_1C_3+C_4\right)+3\beta M\left(2C_3+Mh_1C_4\right)\right)\cosh Mh_1\right),$$

$$L_4=-\frac{3M^5(n-1)}{64}\left(\left(C_3\left(C_3^2+3C_4^2\right)+3\beta MC_4\left(C_4^2+3C_3^2\right)\right)\sinh 3Mh_2+\left(C_4\left(C_4^2+3C_3^2\right)+3\beta MC_3\left(C_3^2+3C_4^2\right)\right)\cosh 3Mh_2\right.$$
$$\left.-\frac{3M^5(n-1)}{16}\left(C_3^2-C_4^2\right)\left(\left((C_3+Mh_1C_4\right)+3\beta M\left(Mh_1C_3+2C_4\right)\right)\sinh Mh_2+\left(\left(Mh_1C_3+C_4\right)+3\beta M\left(2C_3+Mh_1C_4\right)\right)\cosh Mh_2\right),$$

$$L_5=\frac{\left(\sinh Mh_1-\sinh Mh_2\right)^2-\left(\cosh Mh_1-\cosh Mh_2\right)^2}{\left(\sinh Mh_1-\sinh Mh_2\right)},$$

$$L_6=L_1-L_2-\frac{\left(L_3-L_4\right)\left(\cosh Mh_1-\cosh Mh_2\right)}{M\left(\sinh Mh_1-\sinh Mh_2\right)},$$

$$L_7=\frac{L_5}{\left(h_1-h_2\right)}+\frac{M\left(\cosh Mh_1-\cosh Mh_2\right)\left(\sinh Mh_1+\beta M\cosh Mh_1\right)}{\left(\sinh Mh_1-\sinh Mh_2\right)}-M\left(\cosh Mh_1+\beta M\sinh Mh_1\right),$$

$$L_8=L_3-\frac{L_6}{\left(h_1-h_2\right)}-\frac{\left(L_3-L_4\right)\left(\sinh Mh_1+\beta M\cosh Mh_1\right)}{\left(\sinh Mh_1-\sinh Mh_2\right)},$$

$$L_9=\frac{M^3}{2}\left[C_3\left(MC_7-\frac{3}{8}M^5(n-1)C_3\left(C_3^2-C_4^2\right)-\frac{9}{64}M^5(n-1)C_3\left(C_3^2+3C_4^2\right)\right)\right.$$
$$\left.+C_4\left(MC_8-\frac{3}{8}M^5(n-1)C_4\left(C_3^2-C_4^2\right)+\frac{9}{64}M^5(n-1)C_4\left(C_4^2+3C_3^2\right)\right)\right],$$

$$L_{10}=-\frac{3}{16}M^9(n-1)C_3C_4\left(C_3^2-C_4^2\right),$$

$$L_{11}=\frac{M^4}{2}\left(C_3C_8-C_4C_7-\frac{11}{64}M^4(n-1)C_3C_4\left(C_3^2-C_4^2\right)\right),$$

$$L_{12}=-\frac{3}{16}M^5(n-1)\left(C_3^4-C_4^4\right),$$

$$L_{13}=-\frac{9}{128}M^8(n-1)\left(C_3^4+C_4^4+6C_3^2C_4^2\right),$$

$$L_{14}=-\frac{9}{32}M^8(n-1)C_3C_4\left(C_3^2+C_4^2\right),$$

$$L_{15}=\frac{M^4}{2}\left(C_3C_7-C_4C_8-\frac{3}{8}M^5(n-1)\left(C_3^2-C_4^2\right)^2\right),$$

$$L_{16}=\frac{1}{2}\left(C_3^4-C_4^4\right),\quad L_{17}=C_3C_4\left(C_3^2-C_4^2\right),$$

$$L_{18}=\frac{1}{8}\left(C_3^4+C_4^4+6C_3^2C_4^2\right),$$

$$L_{19}=\frac{1}{2}C_3C_4\left(C_3^2+C_4^2\right),\ L_{20}=\frac{3}{8}\left(C_3^4-C_4^4\right)^2.$$

6. Expressions for wave shapes :

The non-dimensional expressions for the five considered wave forms are given by the following equations:

I. Sinusoidal wave:

$$h_1(x)=1+a\sin(2\pi x), \tag{44}$$

$$h_2(x)=-d-b\sin(2\pi x+\phi), \tag{45}$$

II. Triangular wave:

$$h_1(x)=1+a\left\{\frac{8}{\pi^3}\sum_{m=1}^{\infty}\frac{(-1)^{m+1}}{(2m-1)^2}\sin[(2m-1)x]\right\}, \tag{46}$$

$$h_2(x)=-d-b\left\{\frac{8}{\pi^3}\sum_{m=1}^{\infty}\frac{(-1)^{m+1}}{(2m-1)^2}\sin[(2m-1)x+\phi]\right\}, \tag{47}$$

III. Square wave:

$$h_1(x)=1+a\left\{\frac{4}{\pi}\sum_{m=1}^{\infty}\frac{(-1)^{m+1}}{(2m-1)}\cos[(2m-1)x]\right\}, \tag{48}$$

$$h_2(x)=-d-b\left\{\frac{4}{\pi}\sum_{m=1}^{\infty}\frac{(-1)^{m+1}}{(2m-1)}\cos[(2m-1)x+\phi]\right\}, \tag{49}$$

IV. Trapezoidal wave:

$$h_1(x)=1+a\left\{\frac{32}{\pi^2}\sum_{m=1}^{\infty}\frac{\sin\frac{\pi}{8}(2m-1)}{(2m-1)^2}\sin[(2m-1)x]\right\}, \tag{50}$$

$$h_2(x)=-d-b\left\{\frac{32}{\pi^2}\sum_{m=1}^{\infty}\frac{\sin\frac{\pi}{8}(2m-1)}{(2m-1)^2}\sin[(2m-1)x+\phi]\right\}. \tag{51}$$

V. Sawtooth wave:

$$h_1(x)=1+a\left\{\frac{8}{\pi^3}\sum_{m=1}^{\infty}\frac{\sin[2\pi mx]}{m}\right\}, \tag{52}$$

$$h_2(x)=-d-b\left\{\frac{8}{\pi^3}\sum_{m=1}^{\infty}\frac{\sin[2\pi mx+\phi]}{m}\right\}. \tag{53}$$

7. Results and Discussion

In this section results are presented and discussed for different physical quantities of interest. The temperature field for different values of the mean volume flow rate $\overline{Q}$, partial slip β, Weissenberg number *We* and brinkman number *Br* are shown in Figs. 1. It is observed from the figures that the increase in $\overline{Q}$, *We* and *Br* the temperature field increases while with the increase in β, the temperature field decreases. In Figs. 2, the axial velocity distribution is shown for different parameters the mean volume flow rate $\overline{Q}$ and Hartmann number *M*. In Fig. 2(a) we found that the mean flow rate increase with increases the magnitude of the axial velocity and in Fig. 2(b) the magnitude of the axial velocity decreases in the center and increases nearer at the walls of the channel with increasing the Hartmann number *M*. Figs. 3 analyzes the R_m magnetic Reynolds number, *E* the Eckert number, volume flow rate $\overline{Q}$ and partial slip β on the axial induced magnetic field. We observed that an axial magnetic field h_x decreases by increasing Reynolds magnetic number R_m, Eckert number

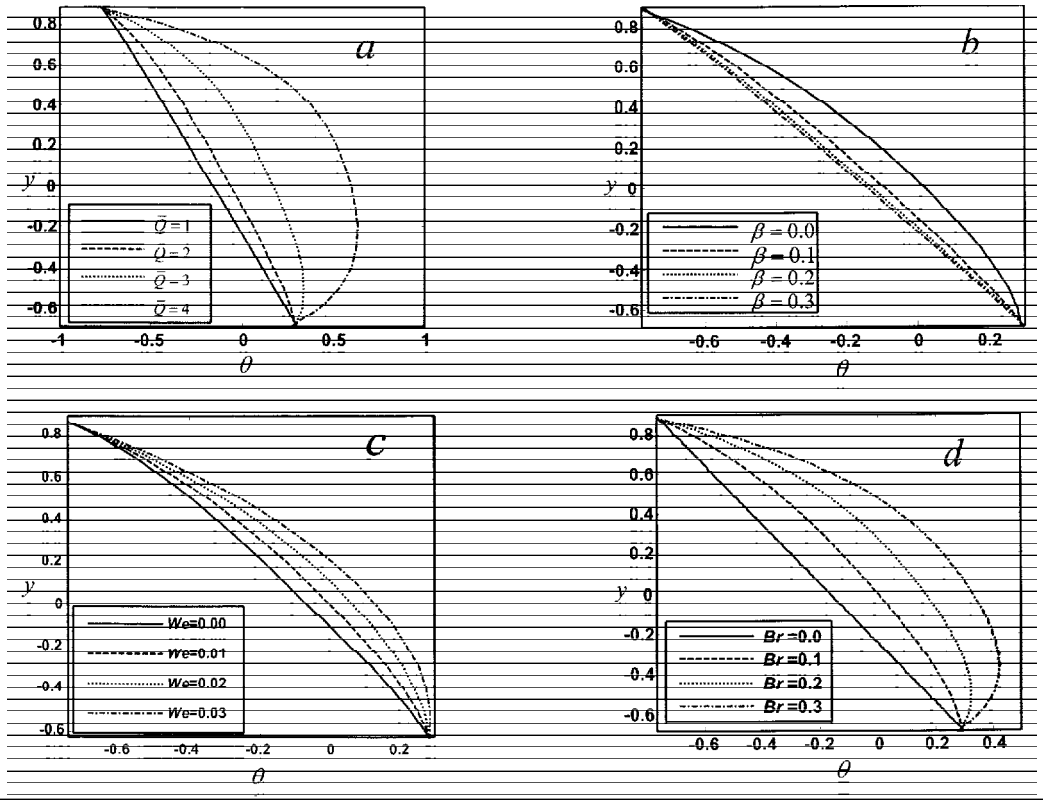

Fig. 1. Temperature distribution θ versus y for a =0.5, b =0.5, d =1, x =0.3, $\phi=\pi/6$, (a) M=1, $\beta=0.01$, n =0.398, Br=0.1, We=0.001; (b) M=1, $\bar{Q}=2$, n =0.398, Br=0.1, We=0.001; (c) M=1, $\beta=0.01$, n =0.398, Br=0.1, $\bar{Q}=2$; (d) M=1, $\beta=0.01$, n =0.398, $\bar{Q}=2$, We=0.001

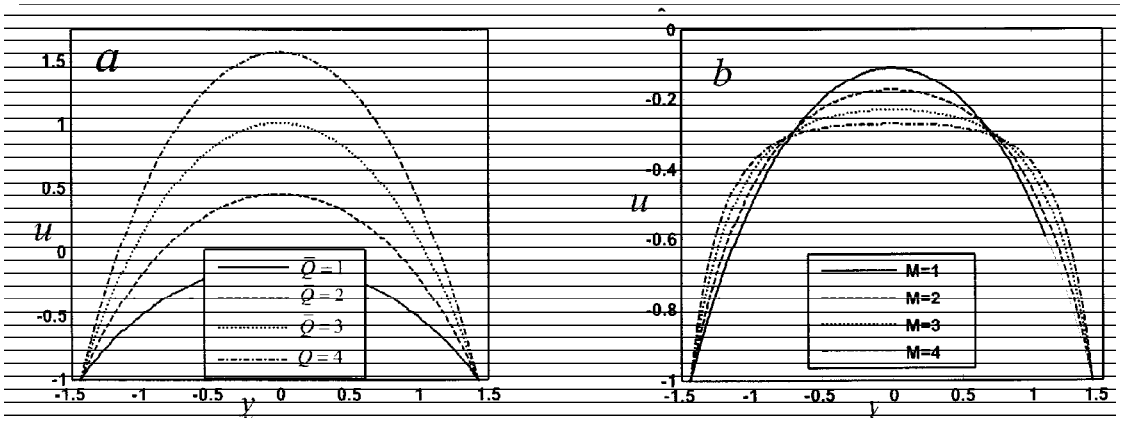

Fig. 2: The axial velocity u with y for a =0.43, b =0.5, d =1, x =1, $\phi=\pi/6$, We=0.001, $\beta=0.001$, n =0.398 ;(a) M=1; (b) $\bar{Q}=2$

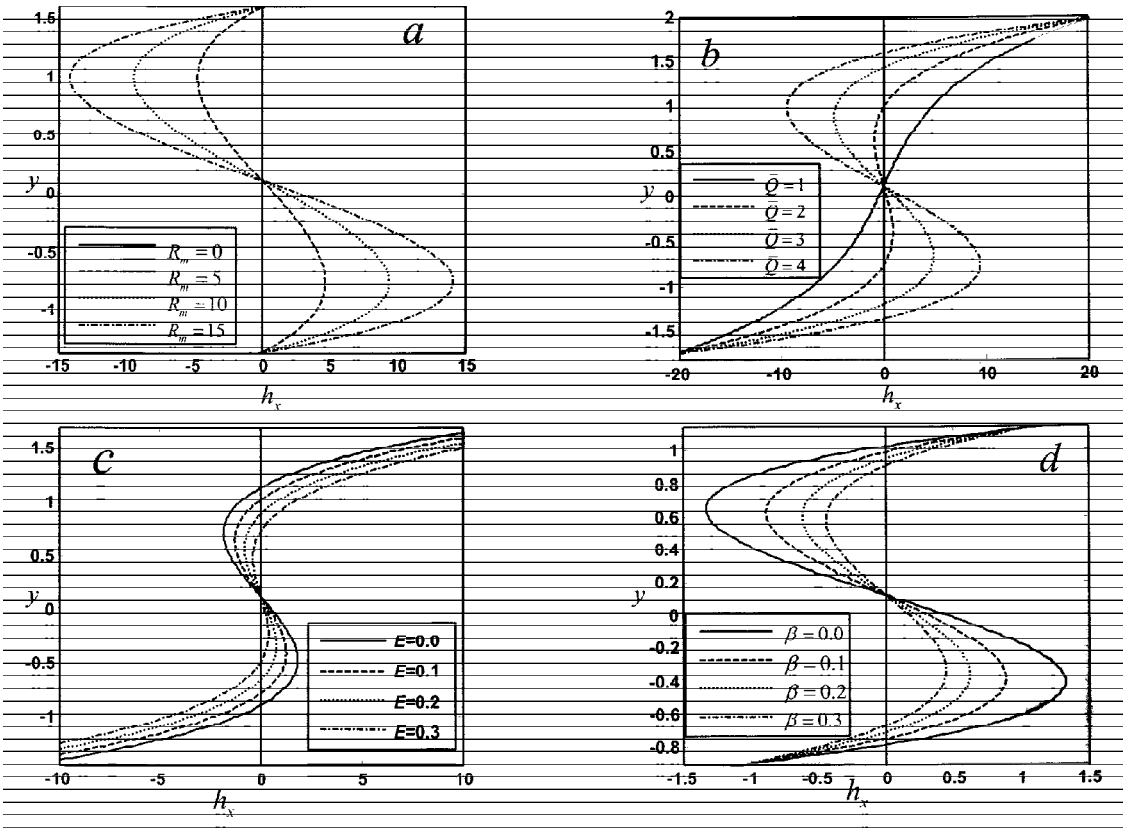

Fig. 3. Axial induced magnetic field h_x versus y for a =0.5, b =0.5, d =1, $\phi=\pi/6$, We= 0.001, x =0.2, n 0.398; (a) $\bar{Q}$ =1, E=0.1, β = 0.01: (b) $\bar{Q}$ =1, β = 0.01, R_m =10 ; (c) β = 0.01, R_m =10, E=0.1; (d) R_m =10 , E=0.1, Q =1.

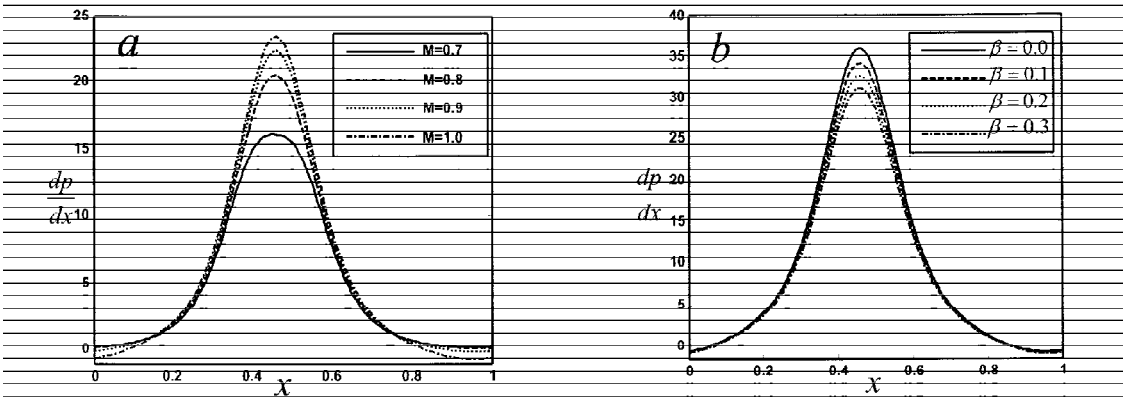

Fig. 4: The pressure distribution dp/dx with x for a 0.5, b =0.5, d =1, $\bar{Q}$ = 2, We=0.001, $\phi=\pi/6$, n =0.398; (a) β = 0.01; (b) M=1.

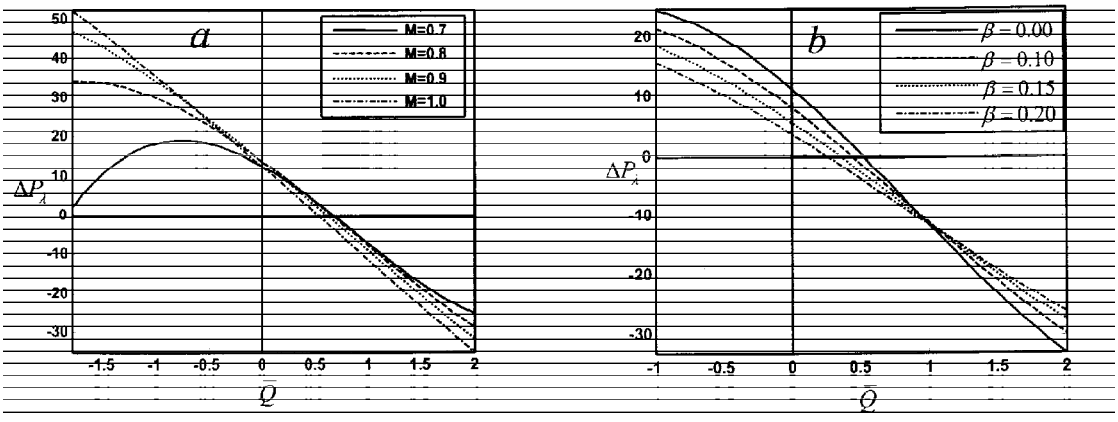

Fig. 5: The pressure rise ΔP_λ with $\bar{Q}$ for a =0.5, b =0.5, d =1, $\phi = \pi/6$, We=0.001, ε =0.1, n =0.398; (a) β = 0.01; (b) M=1.

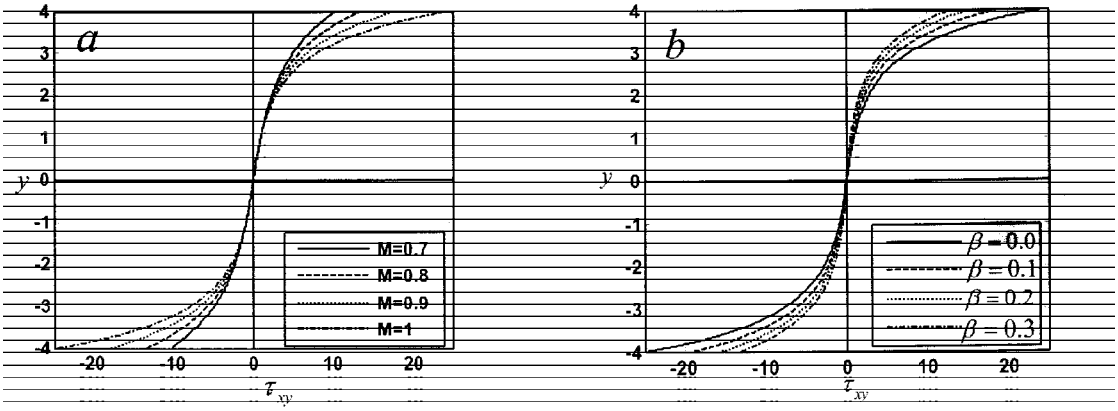

Fig. 6: The shear stress τ_{xy} with y for a =0.5, b =0.5, d =1, $\bar{Q}$ = 2 , x =1, $\phi = \pi/6$, We=0.001, n =0.398; (a) β = 0.01; (b) M=1.

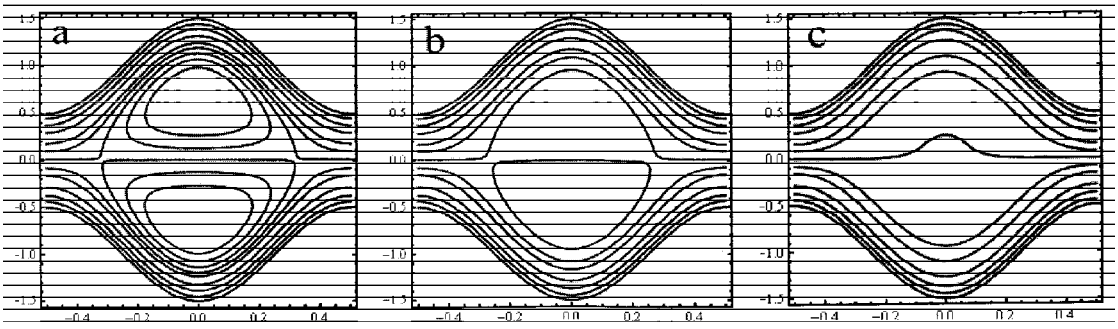

Fig. 7: The stream lines for a =0.5, b =0.5, d =1, Q = 1.5 , ϕ = 0 , We=0.001, n =0.398, β = 0.01; (a) M=1; (b) M=3; (c) M=3.5.

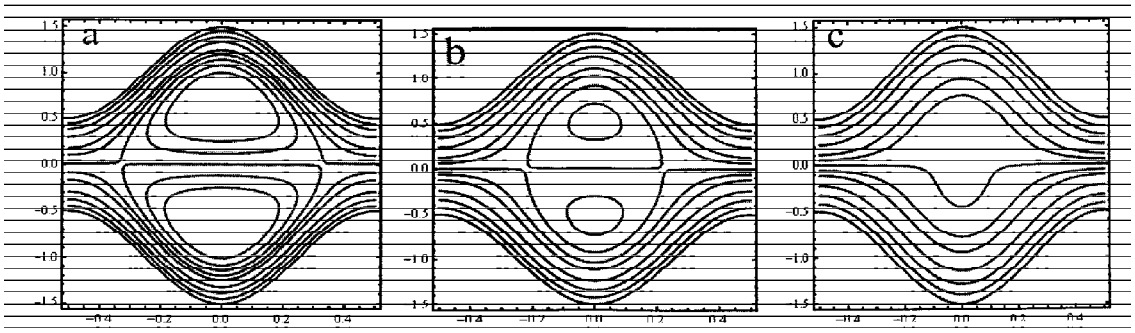

Fig. 8: The stream lines for a =0.5, b =0.5, d =1, $\bar{Q}$ =1.5 , ϕ = 0 , n =0.398, M=1, We=0.001; (a) β = 0.00 ; (b) β = 0.25 ; (c) β = 0.5

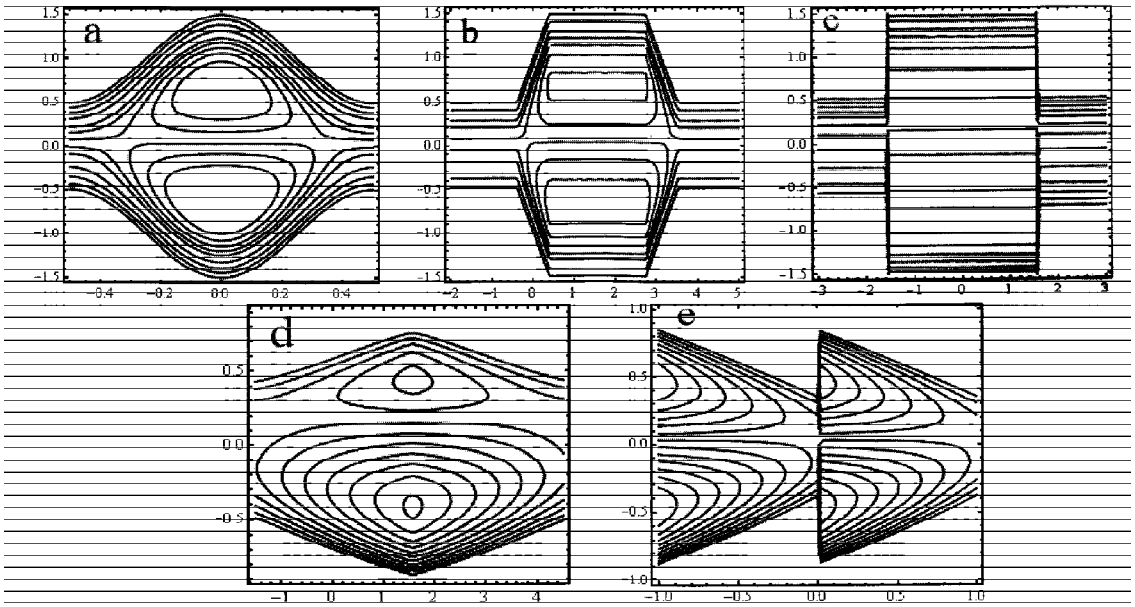

Fig. 9: The stream lines for a =0.5, b =0.5, d =1, Q =1.5 , ϕ = 0 , n =0.398, M=1, We=0.001, β = 0.00 : (a) Sinusoidal; (b) Trapeziodal; (c) Square; (d) Triagulr; (e) Sawtooth waves.

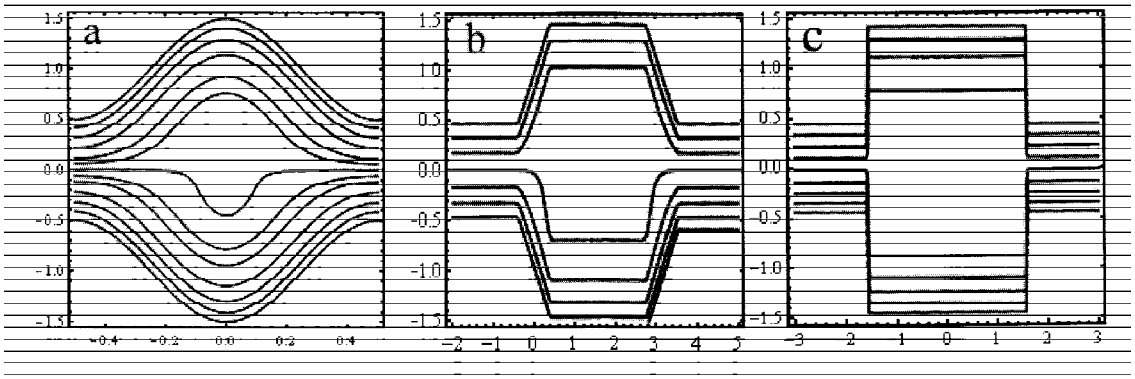

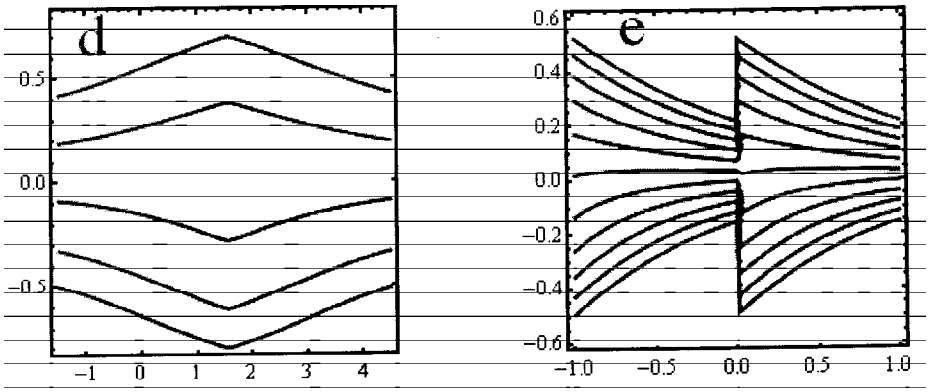

Fig. 10: The stream lines for a =0.5, b =0.5, d =1, $\bar{Q}$ = 1.5 , ϕ = 0 , n =0.398, M=1, We=0.001; β = 0.01, (a) Sinusoidal; (b) Trapeziodal; (c) Square; (d) Triagular; (e) Sawtooth waves.

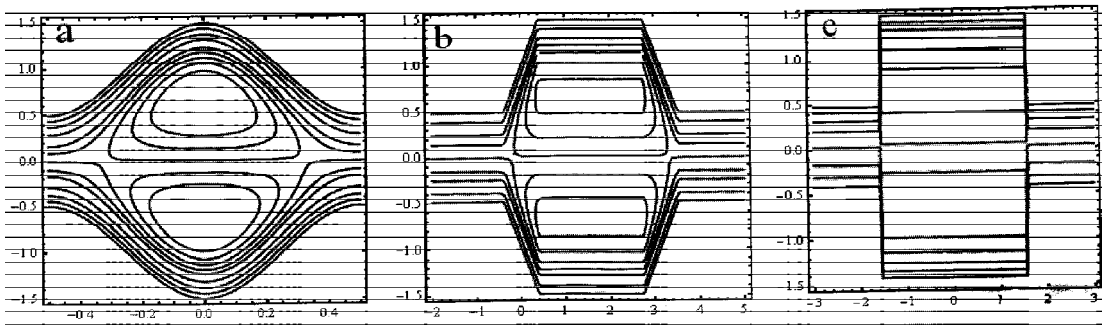

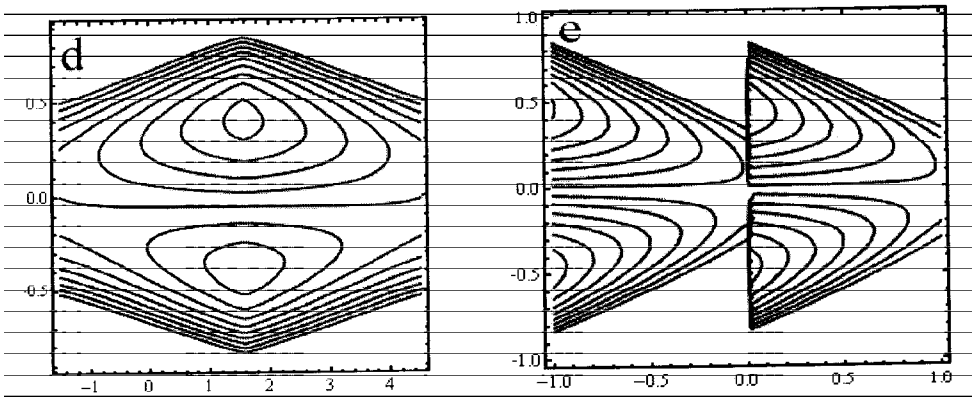

Fig. 11: The stream lines for a =0.5, b =0.5, d =1, $\bar{Q}$ = 1.5 , M=1, ϕ = 0 , M=1, We=0.001; β=0.01, n =1(Newtonian Fluid); (a) Sinusoidal; (b) Trapeziodal; (c) Square; (d) Triagle; (e) Sawtooth waves.

E and partial slip β are in one direction in some part of region where as in other part are in opposite direction in Figs. 3(a)-3(c) and also we have seen in Fig. 3(d) behavior of volume flow rate $\overline{Q}$ is reverse.

Figs. 4 are plotted to see the effect of the parameters *M* and β on the pressure gradient *dp/dx*. *x*=0.5. Fig. 4(a) indicates that the pressure gradient *dp/dx* increases with increasing Hartmann number *M* and the maximum pressure gradient is also near *x*=0.5. Fig. 4(b) show that the pressure gradient *dp/dx* decreases with increasing the partial slip β. Figs. 5 are graphs of the dimensionless pressure rise ΔP_λ versus the variation of time-average flux $\overline{Q}$. The graphs is sectored so that the quadrant (I) designated as region the peristaltic pumping ($\overline{Q}>0$ and $\Delta P_\lambda > 0$). Quadrant (II) is denotes the augmented flow when $\overline{Q}>0$ with $\Delta P_\lambda < 0$. Quadrant (IV) such that $\overline{Q}<0$ and $\Delta P_\lambda > 0$ is called retrograde (or) backward pumping. It is shows that there is a nonlinear relation ΔP_λ versus $\overline{Q}$. Fig. 5(a) is a graph of the pressure rise ΔP_λ per wavelength versus the mean flow rate $\overline{Q}$ of the asymmetric channel for fixed values of other parameters. We observed that an increase in the Hartmann number *M* result decreases in the peristaltic pumping rate and also in an increase in the pressure rise. Fig 5(b) show the variation of pressure rise ΔP_λ with flow rate $\overline{Q}$ for values of partial slip. We observe that the peristaltic pumping rate decrease with increase β. The variation of the axial shear stress τ_{xy} with *y* is calculated from Eq. (43) and is shown in Figs. 6 for different physical parameters. In Figs. 6(a) we observed that the curves intersect at origin and the axial shear stress τ_{xy} decreases with increasing the Hartmann number *M* in the upper wall and an opposite behavior is observed in the lower wall of the channel. The relation between the shear stress τ_{xy} and *y* at different values the partial slip parameter β is depicted in Fig. 6 (b).

7.1 Trapping phenomena :

Another interesting phenomenon in peristaltic motion is the trapping. It is basically the formation of an internally circulating bolus of fluid by closed stream lines. The trapped bolus will be pushed ahead along the peristaltic waves. The stream lines are calculated form Eq. (38) and plotted in Figs. 7-11. It is shown in Figs. 7 that the size of bolus decreases with increasing the Hartmann number *M* while the bolus disappears for *M*=3.49. Fig. 8 is depicted for various values of the partial slip parameter β, It is found that the volume of the trapping bolus decreases as the partial slip parameter β increases, moreover, the bolus disappears at β=0.5. Figs. 9-11 compare for different wave forms like sinusoidal, triangular, trapezoidal, square and sawtooth wave, it is finally observed that the volume of trapping bolus of the Carreau fluid(n=0.398) large in the upper channel and small in the lower channel but an opposite behavior in the case of the Newtonian fluid (n=1) and also the size of the bolus decreases with increase the partial slip.

Conclusion

In the present note, we have discussed the peristaltic transport of a Carreau fluid under

the effect of magnetic field with partial slip. The two-dimensional governing equations have been modeled and then simplified using the long wave length approximation and then solved by using the perturbation technique. The results are discussed through numerically and graphically. We have concluded the following observations:

- The magnitude of the velocity field increases near the walls and decreases at the center of the channel when increasing the Hartmann number M.
- The pressure gradient decreases with increasing the partial slip parameter β.
- In the peristaltic pumping region the pressure rise decreases with increasing β and M.
- The shear stress distribution decreases in the upper wall and increases in the lower wall of the channel with increasing M and also opposite behavior in β.
- The size of tapping bolus decreases with increase β and M while it disappears at M=3.49 and β=0.5.

References

1. A.H. Shapiro, M.Y. Jaffrin, S.L. Weinberg, peristaltic pumping with long wavelength at low Reynolds number, *J. Fluid Mech. 37*, 799-825 (1969).
2. C. Pozrikidis, A study of peristaltic flow, *J. Fluid Mech. 180,* 515-527 (1987).
   K. Vajravelu, S. Sreenadh, K. Rajanikanth, Chanhoon Lee, Peristaltic transport of a Williamson fluid in asymmetric channels with permeable walls, Nonlinear Analysis: *Real World Applications 13,* 2804-2822 (2012).
3. K. Vajravelu, S. Sreenadh, R. Hemadri reddy, K. Murugesan, Peristaltic transport of a Casson fluid in contact with a Newtonian Fluid in a circular Tube with permeable wall, *International Journal of Fluid Mechanics Research,* Vol. *36(3),* 244-254 (2009).
4. M.V. Subba Reddy, A. Ramachandra Rao, S. Sreenadh, Peristaltic motion of a power-law fluid in an asymmetric channel, Int. *J. Non-Linear Mech. 42,* 1153-1161 (2007).
5. T. Hayat, Nasir Ali, Zaheer Abbas, Peristaltic flow of a mocropolar fluid in a channel with different wave forms, *Phys. Lett, A, 370,* 331-344 (2008).
6. Nasir Ali, T. Hayat, Peristaltic motion of a Carreau fluid in an asymmetric channel, *Applied Mathematics and computation 193,* 535-552 (2007).
7. Kh. S. Mekheimer, Effect of magnetic field on peristaltic flow of a couple stress fluid, *Phys. Lett. A 371,* 4271-4278 (2008).
8. I.R. Rao, K.R. Rajagopal, Some simple flows of a Johnson–Segalman fluid, *Acta Mech. 132,* 209–219 (1999).
9. M. Kothandapani, S. Srinivas, Peristaltic transport of a Jeffrey fluid under the effect of magnetic field in an asymmetric channel. *Int. J Non-linear Mech. 43,* 915-924 (2008).
10. T. Hayat, Niaz Ahmad, N. Ali, Effects of an endoscope and magnetic field on the peristalsis involving Jeffrey fluid, *Communications in Nonlinear Science and Numerical Simulation 13,* 1581–1591 (2008).
11. Y. Wang, T. Hayat, N. Ali, M. Oberlack, Magnetohydrodynamics peristaltic motion of Sisko fluid in a symmetric or asymmetric channel. *Physica A 387,* 347-362 (2008).
12. T. Hayat, Y. Wang, A.M. Siddiqui, K. Hutter, S. Asghar, Peristaltic transport of a third-

order fluid in a circular cylindrical tube, *Math. Models Methods Appl. Sci*. 12, 1691–1706 (2002).
13. S. Srinivas, G. Natarajan, A. Rami Reddy, T.V.K. Iyengar, Peristaltic transport of a viscoelastic fluid with heat transfer, *Far East J. Appl. Math, 8,* 203–216 (2002).
14. Y. Wang, T. Hayat, K. Hutter, Peristaltic flow of a Johnson–Segalman fluid through a deformable tube. *Theoret Comput. Fluid Dyn, 21,* 369–80 (2007).
15. L.M. Srivastava, V.P. Srivastava, Peristaltic transport of blood*: Casson model II, J. Fluid. Mech.* 122, 439-465 (1984).
16. Kh. S. Mekheimer, Peristaltic flow of blood under the effect of magnetic field in a non-uniform channels, *Appl. Math. Comput. 153,* 763–77 (2004).
17. S. Srinivas, M. Kothandapani, The influence of heat and mass transfer of MHD peristaltic flow through a porous space with complaints walls, *Applied Mathematics and Computation 213,* 197-208 (2009).
18. S. Nadeem, Safia Akram, Heat transfer in a peristaltic flow of MHD fluid with partial slip, *Commun Nonlinear Sci Numer Simulat 15,* 312–321 (2010).
19. A. Ebaid, Effects of magnetic field and wall slip condition on the peristaltic transport of a Newtonian fluid in asymmetric channel, *Physics letters A 372,* 4493-4499 (2008).
20. S. Nadeem, S. Akram, Heat transfer in a peristaltic flow of MHD fluid with partial slip, *Communications in Nonlinear Science and Numerical Simulation 15,* 312–321 (2010).
21. T. Hyat, Q. Hussain, N. Ali, Influence of the partial slip on the peristaltic flow in a porous medium, *Physica A 387,* 3399–3409 (2008).
22. M. Kothandapani, S. Srinivas, On the influence of wall properties in the MHD peristaltic transport with heat transfer and porous medium, *Phys. Lett. A 372,* 4586–4591 (2008).
23. Mekheimer KhS, Abd elmaboud Y. The influence of heat transfer and magnetic field on peristaltic transport of a Newtonian fluid in a vertical annulus: application of an endoscope. *Phys Lett A 372,* 1657–65 (2008).
24. Kothandapani M., Srinivas S. On the influence of wall properties in the MHD peristaltic transport with heat transfer and porous medium, *Phys Lett A 372,* 4586–91 (2008).
25 T. Hayat, Najma Saleem, S. Asghar, Mohammed Shabab Alhothuali, Adnan Alhomaidan, Influence of induced magnetic field and heat transfer on peristaltic transport of a Carreau fluid, *Commun Nonlinear Simulat, 16,* 3559-3577 (2011).